116 (1990); O. I. Olopade *et al.*, *Proc. Am. Assoc. Cancer Res.* **52**, 1814 (abstr.) (1991); O. I. Olopade *et al.*, *Genomics* **14**, 437 (1992).
17. D. J. Kwiatkowski and M. O. Diaz, *Hum. Molec. Genet.*, in press.
18. N. Hayward, personal communication.
19. The PCR reaction was done with a Perkin Elmer 9600 thermal cycler on genomic DNA (30 ng) with 3 pmol of each oligonucleotide primer. The samples were processed as described [J. L. Weber and P. E. May, *Am. J. Hum. Genet.* **44**, 388 (1989)] except that dCTP was 5 μM with 2.5 μCi [α^{32}P]dCTP. Samples were cycled 27 times at 94°C for 10 s, 55°C for 10 s, and 72°C for 10 s.
20. E. B. Claus, N. Risch, W. D. Thompson, *Am. J. Hum. Genet.* **48**, 232 (1991).
21. D. F. Easton, personal communication; _____ and J. Peto, *Cancer Surv.* **9**, 395 (1990).
22. D. Weeks and K. Lange, *Am. J. Hum. Genet.* **50**, 859 (1992).
23. The strength of evidence for linkage is measured by the lod score, or the $\log_{10}$ of the ratio of the likelihood at a particular recombination fraction to the likelihood at a recombination fraction of 0.5 (representing lack of linkage). A lod score of 3.00 represents odds of about 1000:1 in favor of linkage.
24. G. M. Lathrop, J. M. Lalouel, C. Julier, J. Ott, *Proc. Natl. Acad. Sci. U.S.A.* **81**, 3443 (1984).
25. J. Ott, *Analysis of Human Genetic Linkage* (Johns Hopkins Univ. Press, Baltimore, 1985).
26. W. H. Clark *et al.*, *Arch. Dermatol.* **114**, 732 (1978); H. T. Lynch *et al.*, *J. Med. Genet.* **15**, 352 (1978).
27. M. H. Greene *et al.*, *Ann. Int. Med.* **102**, 458 (1985).
28. NIH Consensus Panel on Early Melanoma, *J. Am. Med. Assoc.* **268**, 1314 (1992).
29. D. E. Goldgar *et al.*, *J. Natl. Cancer Inst.* **83**, 1726 (1991); some of the linkage kindreds were included in this earlier study.
30. L. Pascoe, *Am. J. Hum. Genet.* **40**, 464 (1987); H. Traupe *et al.*, *Am. J. Med. Genet.* **32**, 155 (1989); R. Happle *et al.*, *J. Am. Acad. Dermatol.* **6**, 540 (1982).
31. A. J. Swerdlow *et al.*, *Lancet* ii, 168 (1984).
32. M. H. Greene *et al.*, *Proc. Natl. Acad. Sci. U.S.A.* **80**, 6071 (1983).
33. S. J. Bale *et al.*, *N. Engl. J. Med.* **320**, 1367 (1989).
34. A. van Haeringen *et al.*, *Genomics* **5**, 61 (1989); L. A. Cannon-Albright *et al.*, *Am. J. Hum. Genet.* **46**, 912 (1990); N. A. Gruis *et al.*, *N. Engl. J. Med.* **322**, 853 (1990); R. F. Kefford *et al.*, *Cancer Genet. Cytogenet.* **51**, 45 (1991); D. J. Nancarrow *et al.*, *Genomics* **12**, 18 (1992).
35. S. J. Bale and N. C. Dracopoli, *J. Natl. Cancer Inst.* **81**, 70 (1989).
36. A. J. Sober, R. A. Lew, H. K. Koh, R. L. Barnhill, *Dermatol. Clinics* **9**, 617 (1991).
37. M. Skolnick, in *Cancer Incidence in Defined Populations*, J. Cairns *et al.*, Eds. (Cold Spring Harbor Laboratory, Cold Spring Harbor, NY, 1980), pp. 285–297.
38. Supported by NIH grants CA 48711, RR 00064, CA 42014, CA 54936, CN 05222, CA08985, HG00297, and CA17575; Veterans Administration (L.J.M.), and American Heart Association (D.J.K.). We thank M. Jost, D. Harrison, M. Ashton, T. D. Tran, G. Linker, and D. Housman.

11 September 1992; accepted 19 October 1992

A Functional Connection Between the Pores of Distantly Related Ion Channels as Revealed by Mutant K^+ Channels

Lise Heginbotham, Tatiana Abramson, Roderick MacKinnon

The overall sequence similarity between the voltage-activated K^+ channels and cyclic nucleotide–gated ion channels from retinal and olfactory neurons suggests that they arose from a common ancestor. On the basis of sequence comparisons, mutations were introduced into the pore of a voltage-activated K^+ channel. These mutations confer the essential features of ion conduction in the cyclic nucleotide–gated ion channels; the mutant K^+ channels display little selectivity among monovalent cations and are blocked by divalent cations. The property of K^+ selectivity is related to the presence of two amino acids that are absent from the pore-forming region of the cyclic nucleotide–gated channels. These data demonstrate that very small differences in the primary structure of an ion channel can account for extreme functional diversity, and they suggest a possible connection between the pore-forming regions of K^+, Ca^{2+}, and cyclic nucleotide–gated ion channels.

Ion channels are integral membrane proteins that form ion conduction pathways across cell membranes. The channel-mediated movement of ions into and out of cells underlies a variety of cellular functions such as muscle contraction, cell volume regulation, and the production of electrical signals in the nervous system. In order to fill their many different roles the ion channels are a diverse class of proteins. Some ion channels open in response to a change in membrane electrical potential, and others open in response to the binding of specific ligands. After having opened, some ion channels are not very selective and allow many different ions to pass, but others are highly selective and allow the conduction of only one kind of ion present in physiological solutions.

The voltage-activated Na^+, Ca^{2+}, and K^+ channels are members of the same gene superfamily; they open and close in response to membrane electrical potential and they are similar in their primary structures (*1*). The most characteristic structural feature shared by members of this superfamily is an amino acid segment called S4, which is an unusual stretch of hydrophobic and basic amino acids that is thought to serve as a transmembrane voltage sensor for channel gating (*2*).

The cyclic nucleotide–gated ion channels (CNG channels) from olfactory and retinal neurons are unexpected members of the S4-containing superfamily of ion channels (*3*, *4*). Unlike the voltage-activated channels, the CNG channels open and close in response to the binding of an intracellular ligand. Nevertheless, their amino acid sequences reveal a distant ancestral connection to the voltage-activated ion channels. In addition to having a residual S4 sequence (*5*), the CNG channels also contain a pore-forming region (P region) that bears a striking resemblance to the equivalent region of the K^+ channels (*6*, *7*).

The sequence similarity between voltage-activated K^+ channels and CNG channels is intriguing because they are functionally so dissimilar. The P regions are conserved (Fig. 1A), yet the ion conduction properties of these channels are not at all alike. The CNG channels do not discriminate between the alkali metal cations Na^+ and K^+; both are highly permeant (*8*, *9*). Furthermore, the CNG channels are blocked by the divalent cations Ca^{2+} and Mg^{2+} (*9*, *10*). The K^+ channels, in contrast, are highly selective for K^+ over Na^+, and they are not efficiently blocked by Ca^{2+} or Mg^{2+}.

We have identified the essential feature that distinguishes the pore regions of the voltage-activated K^+ channels from the CNG ion channels. The different ion conduction properties can be explained in terms of two amino acids that are present in K^+-selective channels and absent from CNG ion channels. These results demonstrate a close relationship between ion channels that are functionally different, and they show how the interconversion of one kind of ion conduction pore to another might have occurred in nature.

An alignment of the P region of a Shaker K^+ channel with the corresponding region of the bovine retinal CNG channel shows that the sequences between amino acid residues 434 and 444 are highly similar (Fig. 1A) (*11*). To the right of Gly^{444} we introduced a gap and aligned the Glu (E) of the CNG channel with the Asp (D) of the Shaker K^+ channel (*12*). This choice of sequence alignment implies that the CNG channel is missing two amino acids that are present in the K^+ channel pore.

Two mutant K^+ channels were designed such that their pore sequences would mimic that of the CNG channel. The first (Chimera, Fig. 1A) replaces YGDMTPV (resi-

Department of Neurobiology, Harvard Medical School, Boston, MA 02115.

dues 445 to 451) of the Shaker K^+ channel with ETPPP. The second mutation (Deletion, Fig. 1A) deletes residues YG from the P region of the Shaker K^+ channel. Both mutant channels produced voltage-activated currents in *Xenopus* oocytes (Fig. 1, C and D). The gating properties were significantly altered; most notable was the slow rate of activation during the depolarizing pulse as compared to the wild-type Shaker K^+ channel (Fig. 1B). However, the very basic property of voltage activation with membrane depolarization was preserved (Fig. 1E).

Inspection of the currents carried by the chimera (Fig. 1C) and the deletion mutant (Fig. 1D) reveals that these ion channels are no longer selective for K^+. The recordings were made in the absence of extracellular K^+; thus the inward current at negative membrane potentials was carried by Na^+. In particular, the large tail currents present at −110 mV immediately after the depolarizing pulses reflected inward Na^+ current. In contrast, for the wild-type Shaker K^+ channel no inward tail currents were observed in the absence of extracellular K^+ (Fig. 1B).

A more detailed investigation illustrated that the deletion mutant channel displays little selectivity among the alkali metal cations. The smallest of these cations, Li^+, carried a large inward current (Fig. 2A). With Li^+, Na^+, K^+, or Cs^+ as the sole monovalent cation in the bath solution, the reversal potential of the current generated by the deletion mutant channel was within 20 mV of zero (Fig. 2C). In contrast to the alkali metal cations, the large organic cation tetramethylammonium (TMA^+) appeared to be completely impermeant (Fig. 2B). Moreover, the mutant channel is still selective for cations over Cl^- because all inward current was abolished when the impermeant cation TMA^+ was present in the extracellular solution (Fig. 2B).

Blockade by divalent cations is characteristic of the ion conduction pore of CNG channels (*9*, *10*). The deletion mutant is also blocked by divalent cations. When Ca^{2+} and Mg^{2+} were added to the extracellular solution, the ionic currents were almost completely inhibited (Fig. 3, A and B). The inhibition constant for Ca^{2+}, measured during the tail current at −110 mV, is 38 μM (Fig. 3, C and D). External Mg^{2+} also blocks the currents but with much lower affinity (K_i = 418 μM, Fig. 3D). Wild-type Shaker K^+ channels, in contrast, are relatively insensitive to millimolar concentrations of external Ca^{2+} or Mg^{2+} (Fig. 3D). Thus the deletion mutation not only has resulted in the loss of K^+ selectivity but also has created a relatively high-affinity Ca^{2+} and Mg^{2+} blocking site in the ion channel pore.

The newly acquired sensitivity to Ca^{2+} and Mg^{2+} provides the most convincing evidence that the deletion mutant may truly mimic the CNG channel pore. On the basis of structures of proteins containing Ca^{2+} binding sites one might expect Asp^{447} in the pore of the deletion mutant channel (and the corresponding Glu in the CNG channel) to influence the binding of a divalent cation (*13*). Several derivatives of the deletion mutant channel were produced by replacing Asp^{447} with other amino acids. Of the substitutions made—Glu, Asn, Phe, Ser, His, Cys, and Val—only the derivative mutant with Glu produced functional channels in oocytes (Fig. 4, A and B). When Glu is present, Ca^{2+} inhibits the channel with a K_i of only 5.9 μM (Fig. 4, C and D). This result suggests that the acidic residue at position 447 may line the pore of the deletion mutant channel.

To investigate the current amplitude of individual deletion mutant channels, we recorded currents from an excised macropatch that contained many channels. The resulting

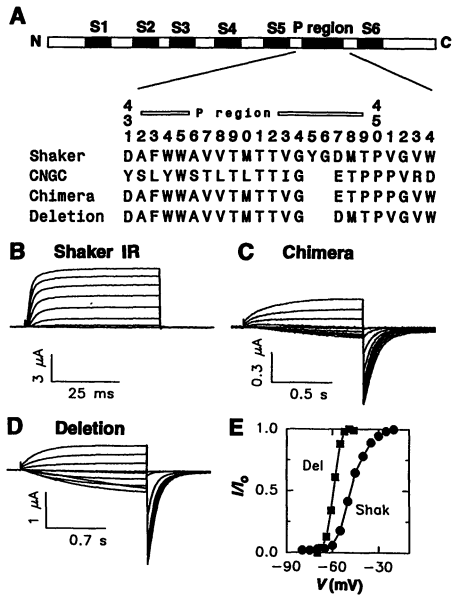

Fig. 1. (**A**) Schematic diagram of the proposed membrane topology of the Shaker K^+ channel. Presumed intramembrane regions are shaded; the S1–S6 segments were initially identified by hydropathy analysis (*20–22*), and the P region has been defined by functional characteristics (*14*, *23*). The deduced amino acid sequences of the P region from the Shaker channel (Shaker) (*20*), the analogous region of the CNG cation channel from bovine retina (CNGC) (*3*), and the sequences of two Shaker channel mutants (Chimera and Deletion) are illustrated. Although these mutations were introduced into Shaker IR (*24*), the wild-type amino acid numbering has been retained (*25*). (**B**) Macroscopic currents recorded from a *Xenopus* oocyte injected with RNA coding for Shaker IR. Currents were recorded using the cut-open oocyte clamp (*26*), with external and guard solutions of 100 mM NaCl, 1 mM $CaCl_2$, 1 mM $MgCl_2$, 5 mM Hepes-NaOH (pH 7.6), and an internal solution of 100 mM KCl, 5 mM EGTA, 1 mM $MgCl_2$, 5 mM Hepes-NaOH (pH 7.6). The oocyte was held at a potential of −90 mV, and currents were elicited during pulses from −70 mV to +20 mV in 10-mV steps. The tail potential following depolarization was −110 mV. A P/4 pulse protocol was used to subtract leak and capacitive currents (*27*). (**C** and **D**) Currents from oocytes expressing the chimera or deletion mutant channels were recorded using standard two-microelectrode voltage clamp (*28*). The bath solution contained 100 mM NaCl, 1 mM $MgCl_2$, 5 mM EGTA, 5 mM Hepes-NaOH (pH 7.6). The same voltage protocol as in (B) was used but with longer pulse durations. For the mutant channels, leak but not capacitive currents were subtracted from the traces shown (*28*). In uninjected oocytes small endogenous outward currents are observed with depolarizations to positive voltages. We have never observed inward, activating currents (C and D) in uninjected oocytes. (**E**) The voltage dependence of activation of the deletion mutant current (squares) was measured as the fraction of current seen in the tail (normalized to −20 mV, I/I_o) after a 1.5-s activating pulse to the indicated potentials. A similar protocol, with a 50-msec pulse, normalized to the current seen after stepping to 0 mV, yields the curve illustrated for the Shaker IR current (circles).

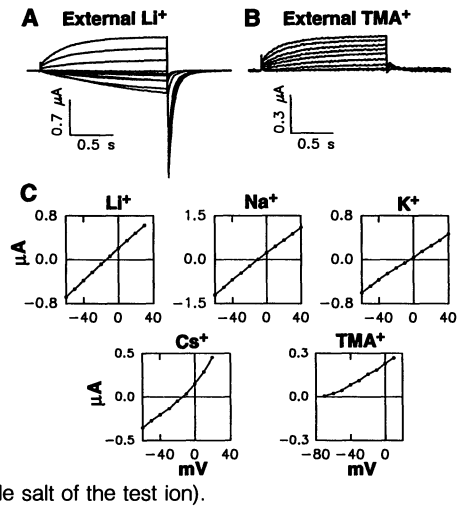

Fig. 2. The deletion mutant channel displays little selectivity among monovalent cations as large as Cs^+. (**A** and **B**) Macroscopic recordings were made from oocytes expressing the deletion mutant channel with 100 mM LiCl (A) or 100 mM TMA-Cl (B) in the bath solution. Currents were elicited by pulses from a holding potential of −90 mV to potentials between −70 and +20 mV (A) or between −70 and +10 mV (B), in 10-mV increments. The oocyte was repolarized with a tail potential to −110 mV. (**C**) Selectivity of the deletion mutant channel was measured using two-microelectrode voltage clamp. Instantaneous *I-V* curves were generated in bath solutions containing the indicated monovalent cation by eliciting current with a step to −20 mV. The bath solution in all experiments contained 5 mM EGTA, 0.1 mM $MgCl_2$, 5 mM Hepes, and 100 mM chloride salt of the test cation (pH was adjusted to 7.6 using the hydroxide salt of the test ion).

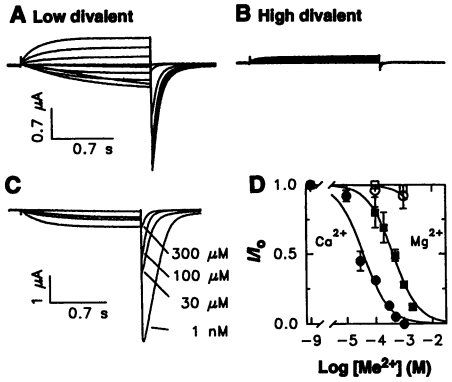

Fig. 3. The deletion mutant channel is blocked by externally applied divalent cations. (**A** and **B**) Currents from the same oocyte expressing the deletion mutant channel were recorded in the presence of either 10^{-9} M Ca^{2+} and 0.5 mM Mg^{2+} (low divalent, A) or 1 mM Ca^{2+} and 1 mM Mg^{2+} (high divalent, B). The holding potential was −90 mV, and currents were elicited by depolarizing pulses from −70 mV to +20 mV, in steps of 10 mV. The tail potential was −110 mV. (**C**) Currents were inhibited by the addition of Ca^{2+} to the bath. Free Ca^{2+} concentrations are indicated. At concentrations less than 100 μM, Ca^{2+} was buffered with EGTA. Mg^{2+} was not added in these experiments. Currents were activated by depolarization from −90 mV to −30 mV, followed by a hyperpolarizing tail potential of −110 mV. (**D**) Fraction of current (I/I_0) remaining after application of the indicated concentrations of either Ca^{2+} (circles) or Mg^{2+} (squares). Blockade of the mutant channels was tested at −110 mV (filled symbols). Blockade of the wild-type Shaker K^+ channel was carried out in 100 mM bath KCl in order to measure blockade of inward K^+ currents at −50 mV (open symbols). The voltage at which blockade was measured in the mutant and wild-type channels does not account for the difference in sensitivity because the mutant channels are blocked very effectively even at −30 mV (C). Each point is the average of three to five measurements made in separate oocytes; error bars show the SD. The curves are fits to a Langmuir isotherm with K_i equal to 38 μM (Ca^{2+}) and 418 μM (Mg^{2+}). Measurements were made using two-microelectrode voltage clamp. For Ca^{2+} titrations the external solution contained 100 mM NaCl, 5 mM EGTA (for $CaCl_2$ less than 100 μM), 10 mM Hepes-NaOH (pH 7.6). For Mg^{2+} titrations the bath contained 100 mM NaCl, 1 mM EDTA (for $MgCl_2$ less than 100 μM), 5 mM Hepes-NaOH (pH 7.6).

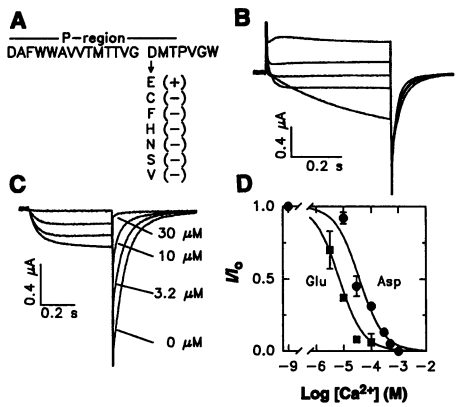

Fig. 4. Mutations of Asp^{447} alter the Ca^{2+} sensitivity of the deletion mutant channel. (**A**) The P region sequence of the deletion mutant channel is shown. Asp (D) was replaced by Glu (E) or one of several uncharged amino acids (arrow). Only the channel with a Glu substitution produced currents in oocytes (+). (**B**) Currents from the D447E deletion mutant channel were measured during depolarizing steps ranging from −70 mV to +10 mV in 20-mV increments from a −90 mV holding potential. The tail potential was −110 mV. The bath solution contained 100 mM NaCl, 5 mM EGTA, 5 mM Hepes-NaOH (pH 7.6). (**C**) Blockade of the D447E deletion mutant channel by Ca^{2+}. Currents were measured at the indicated concentrations of free Ca^{2+} during membrane depolarization to −40 mV followed by hyperpolarization to −110 mV. (**D**) For the deletion mutant channels with an Asp or Glu at position 447, the fraction of current remaining (I/I_0) as a function of the free Ca^{2+} concentration is shown. Currents were measured at a tail potential of −110 mV. Points and error bars represent the means ± SD of three to five determinations in separate oocytes. The curves correspond to Langmuir functions with K_i = 5.9 μM (Glu) and 38 μM (Asp). The bath solutions contained 100 mM NaCl, 5 mM EGTA (for Ca^{2+} less than 100 μM), 5 mM Hepes-NaOH (pH 7.6).

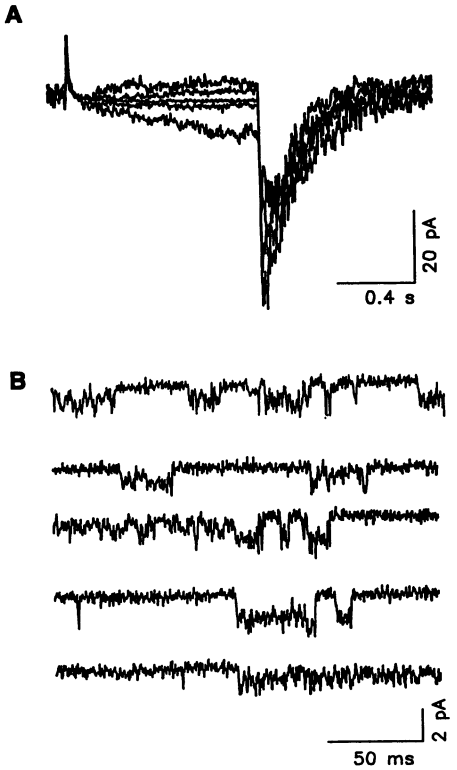

Fig. 5. Patch recordings made from oocytes expressing the deletion mutant channel. (**A**) Macroscopic currents from an inside-out patch were elicited in response to depolarizing pulses from −50 mV to +30 mV in 20-mV increments, from a holding potential of −90 mV. The recording solution on the inside was 100 mM KCl, 1 mM $MgCl_2$, 5 mM EGTA, 10 mM Hepes-KOH and on the outside was 100 mM NaCl, 5 mM EGTA, 10 mM Hepes-NaOH (pH 7.6), with 10 μM (free) Ca^{2+}. (**B**) Single-channel recordings of the deletion mutant channel at −80 mV in outside-out patches were made in symmetric solutions containing 130 mM NaCl, 0.1 mM EDTA, 3 mM Hepes-NaOH (pH 7.6). Data were filtered at 2 kHz and sampled at 5 kHz.

current time course was similar to that observed during the whole oocyte experiments (Fig. 5A). When an excised membrane patch was held at −80 mV, occasional single channel openings were observed (Fig. 5B). The channels were very flickery, and the opening bursts were not uniform. Longer duration, smaller amplitude bursts (fifth trace) were easily distinguished from larger amplitude openings (fourth trace). A transition from one kind of opening to the other within a single burst often occurred (third trace). Nevertheless, the single-channel current amplitude was roughly similar to that of the wild-type Shaker K^+ channel (about −2.0 pA at −80 mV with 100 mM symmetric KCl) (*14*). We conclude that the deletion mutation produced a drastic alteration in the ability of the K^+ channel to select for K^+ over Na^+ ions, yet the absolute ion translocation rate was not altered greatly. Perhaps the steps that govern the rate of ion diffusion through the pore are separate from those mediating ion selectivity. The native CNG channels also have a single-channel conductance (in NaCl) that is within a factor of two of that of the wild-type Shaker K^+ channel (*10*).

A high degree of conservation in the pore-forming region of K^+ channels and CNG channels is surprising because their ion conduction properties are different. But close inspection of the P-region amino acid sequences reveals a fundamental distinction between these channels; K^+-selective channels have in addition the two "extra" amino acids YG between the highly conserved residues 434 to 444 and the aspartate residue (Fig. 1A). The significance of this sequence difference is strengthened by the induction of CNG channel–like ion conduction properties in a K^+ channel through the deletion of these amino acids. Although we have not reconstituted precisely the ion conduction properties of CNG channels, a two–amino acid deletion confers the dominant features. We emphasize that these results do not argue that K^+-selective channels and CNG channels have pores with similar structures. The two amino acid deletion has undoubtedly altered the K^+ channel pore significantly. But even though we do not yet understand the mechanism of how in one case the pore is K^+-selective and in the other it is nonselective and blocked by divalent ions, we can conjecture how nature could transform one into the other through the deletion or insertion of two amino acids.

The results of this study can be examined in the context of several recently cloned K^+ channel genes, *eag* from *Drosophila* and KAT1 and AKT1 from the plant *Arabidopsis thaliana* (*15, 16*). These K^+ channels are more closely related by overall sequence similarity to the CNG channels than to the voltage-activated K^+ channels. They even contain a cyclic nucleotide–binding consensus sequence in their COOH-termini (6, *16*). However, in a single striking way the pore regions of the *Arabidopsis* channels (and *eag*) are more like the voltage-activated K^+ channels; the K^+-selective channels have the familiar sequence GYGD in the COOH-terminal side of the P region (GFGN for *eag*) (Fig. 6A). The two "extra" residues YG are present.

A possible evolutionary connectivity between several functionally distinct classes of ion channels seems to be emerging. The *Arabidopsis* K^+ channels and *eag* (lower left, Fig. 6B) naturally fall in between the voltage-activated K^+ channels (upper left) and the nonselective CNG channels (lower right). It will be interesting to see if this intermediate class of K^+ channels is gated by cyclic nucleotides. [Indeed, a K^+-selective and cAMP-gated channel from *Drosophila* muscle has already been functionally characterized (*17*).]

We now have produced voltage-activated channels that are nonselective for monovalent cations and are blocked by divalent cations. These biophysical properties are very reminiscent of the voltage-activated Ca^{2+} channels (*18*) (Fig. 6B, upper right). In the absence of divalent cations the Ca^{2+} channels conduct monovalent cations nonselectively. Divalent cations at low concentrations block conduction through Ca^{2+} channels. Only at millimolar concentrations of Ca^{2+} does Ca^{2+} conduction occur.

That the K^+ channel deletion mutants are functionally similar to Ca^{2+} channels is intriguing especially in light of the amino acid sequences of the four domains of a Ca^{2+} channel (Fig. 6A). The Gly-Glu pair present in three of the four Ca^{2+} channel domains matches the Gly-Asp pair in the K^+ channel deletion mutant. More importantly, the acidic residues may function similarly in the pore of these two ion channels. We have shown that a mutation of the Asp to Glu alters the Ca^{2+}-blocking affinity almost tenfold. Mutations involving the equivalent residue in Na^+ channels result in Ca^{2+} channel–like ion conduction properties (*19*). Thus the acidic residue influences the way Ca^{2+} interacts with the pores in both ion channels. Although the CNG ion channels are overall more closely related to the K^+ channels than the Ca^{2+} channels, they have served as a missing link in helping us to understand a possible relationship between the pores of K^+ and Ca^{2+} channels.

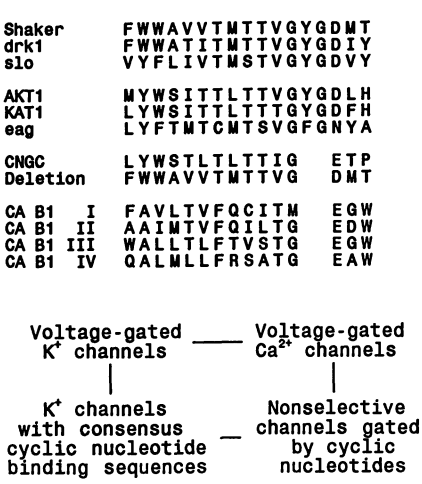

Fig. 6. Alignment of the deduced amino acid sequences of the pore regions of several members of the S4-containing ion channel superfamily. Shaker and drk1 are voltage-activated K^+ channels (*20, 29*); slo is a Ca^{2+}-activated K^+ channel (*30, 31*); AKT1 and KAT1 encode K^+ channels from the plant *Arabidopsis thaliana* (*16*); *eag* is a K^+ channel from *Drosophila* (*15*). AKT1, KAT1, and *eag* contain sequences that are consensus sites for cyclic nucleotide binding domains. CNGC is the CNG channel cloned from bovine retinal neurons (*3*). Deletion is the Shaker IR deletion mutant described in this study. CA B1 I-IV are the homologous regions from the four domains of the brain Ca^{2+} channel (*32*). (**B**) This diagram illustrates the possible evolutionary connectivity relating several members of the S4 ion channel superfamily.

REFERENCES AND NOTES

1. B. Hille, *Ionic Channels of Excitable Membranes* (Sinauer, Sunderland, MA, 1991).
2. W. Stühmer *et al.*, *Nature* **339**, 597 (1989); D. M. Papazian, L. C. Timpe, Y. N. Jan, L. Y. Jan, *ibid.* **349**, 305 (1991); E. R. Liman, P. Hess, F. Weaver, G. Koren, *ibid.* **353**, 752 (1991).
3. U. B. Kaupp *et al.*, *ibid.* **342**, 762 (1989).
4. R. S. Dhallan, K.-W. Yau, K. A. Schrader, R. R. Reed, *ibid.* **347**, 184 (1990).
5. L. Y. Jan and Y. N. Jan, *ibid.* **345**, 672 (1990).
6. H. R. Guy, S. R. Durell, J. Warmke, R. Drysdale, B. Ganetzky, *Science* **254**, 730 (1991).
7. E. H. Goulding *et al.*, *Neuron* **8**, 45 (1992).
8. K.-W. Yau, P. A. McNaughton, A. L. Hodgkin, *Nature* **292**, 502 (1981); A. L. Zimmerman and D. A. Baylor, *J. Physiol.* (*London*) **449**, 759 (1992).
9. T. Kurahashi, *J. Physiol.* (*London*) **419**, 177 (1989).
10. L. W. Haynes, A. R. Kay, K.-W. Yau, *Nature* **321**, 66 (1986); A. L. Zimmerman and D. A. Baylor, *ibid.*, p. 70, K.-W. Yau and D. A. Baylor, *Annu. Rev. Neurosci.* **12**, 289 (1989).
11. The P-region sequence is highly conserved among K^+ channels. For example, the P-region sequence of mammalian Shaker homologs is nearly identical to that shown in Fig. 1A [A. Baumann, A. Grupe, A. Ackermann, O. Pongs, *EMBO J.* **7**, 2457 (1988)]. Potassium channels that are even more distantly related to the Shaker K^+ channel also have a highly conserved P region (Fig. 6).
12. Abbreviations for the amino acid residues are: A, Ala; C, Cys; D, Asp; E, Glu; F, Phe; G, Gly; H, His; I, Ile; K, Lys; L, Leu; M, Met; N, Asn; P, Pro; Q, Gln; R, Arg; S, Ser; T, Thr; V, Val; W, Trp; Y, Tyr.
13. R. H. Kretsinger, *CRC Crit. Rev. Biochem.* **8**, 119 (1980).
14. R. MacKinnon and G. Yellen, *Science* **250**, 276 (1990).
15. J. Warmke, R. Drysdale, B. Ganetzky, *ibid.* **252**, 1560 (1991).
16. H. Sentenac *et al.*, *ibid.* **256**, 663 (1992); J. A. Anderson, S. S. Huprikar, L. V. Kochian, W. J. Lucas, R. F. Gaber, *Proc. Natl. Acad. Sci. U.S.A.* **89**, 3736 (1992).
17. R. Delgado, P. Hidalgo, F. Diaz, R. Latorre, P. Labarca, *Proc. Natl. Acad. Sci. U.S.A.* **88**, 557 (1991).
18. P. Hess and R. W. Tsien, *Nature* **309**, 453 (1984); W. Almers and E. W. McCleskey, *J. Physiol.* (*London*) **353**, 585 (1984).
19. S. H. Heinemann, H. Terlau, W. Stühmer, K. Imoto, S. Numa, *Nature* **356**, 441 (1992).
20. B. L. Tempel, D. M. Papazian, T. L. Schwarz, Y. N. Jan, L. Y. Jan, *Science* **237**, 770 (1987).
21. O. Pongs *et al.*, *EMBO J.* **7**, 1087 (1988).
22. A. Kamb, L. E. Iverson, M. A. Tanouye, *Cell* **50**, 405 (1987).
23. R. MacKinnon, L. Heginbotham, T. Abramson, *Neuron* **5**, 767 (1990); G. Yellen, M. E. Jurman, T. Abramson, R. MacKinnon, *Science* **251**, 939 (1991); A. J. Yool and T. L. Schwarz, *Nature* **349**, 700 (1991); H. A. Hartmann *et al.*, *Science* **251**, 942 (1991); M. P. Kavanaugh *et al.*, *J. Biol. Chem.* **266**, 7583 (1991).
24. The Shaker channel construct (Shaker IR) from which mutations were made is the Shaker H4 channel (*22*) with two alterations. Amino acids 6 to 46 were deleted to remove fast inactivation [T. Hoshi, W. N. Zagotta, R. W. Aldrich, *Science* **250**, 533 (1990)]. In addition, in the Shaker IR used in these experiments a short linking sequence encoding an NCO 1 restriction endonuclease site as well as nine new amino acids (NNNNNNAMV) were added to the COOH-terminus in order to allow future incorporation of these mutations into a tandem dimer construct. These modifications do not alter the ion conduction properties of the wild-type Shaker K^+ channels [L. Heginbotham and R. MacKinnon, *Neuron* **8**, 483 (1992)].
25. Oligonucleotide-directed mutagenesis was performed using the dut^- ung^- method of Kunkel [T. A. Kunkel, *Proc. Natl. Acad. Sci. U.S.A.* **82**, 488 (1985)] and the Mutagene kit (Bio-Rad). Deletions were made with a loop-out oligonucleotide. After confirmation of the mutation using dideoxy sequencing [F. Sanger, S. Nicklen, A. R. Coulson, *Proc. Natl. Acad. Sci. U.S.A.* **74**, 5463 (1977)], we prepared RNA using T7 polymerase. *Xenopus* oocytes were prepared and injected as previously described [R. MacKinnon, P. H. Reinhart, M. M. White, *Neuron* **1**, 997 (1988)]. Two independent colonies of each mutation were prepared and studied.
26. M. Taglialatela, L. Toro, E. Stefani, *Biophys. J.* **61**, 78 (1992).
27. F. Bezanilla and C. M. Armstrong, *J. Gen. Physiol.* **70**, 549 (1977).
28. Oocytes were studied using a two-microelectrode voltage-clamp amplifier (Warner Instruments). A DC leak subtraction was performed by collecting a leak pulse associated with each test protocol. Oocyte membranes become very leaky in the complete absence of divalent cations. Therefore, where possible, channels were studied under a partially blocked state in the presence of Mg^{2+} (concentrations indicated). Due to the extremely slow deactivation of the deletion mutant channel, tail currents were measured at −110 mV to increase the rate of deactivation.
29. G. C. Frech, A. M. J. VanDongen, G. Schuster, A. M. Brown, R. H. Joho, *Nature* **340**, 642 (1989).
30. N. S. Atkinson, G. A. Robertson, B. Ganetzky, *Science* **253**, 551 (1991).
31. J. P. Adelman *et al.*, *Neuron* **9**, 209 (1992).
32. Y. Mori *et al.*, *Nature* **350**, 398 (1991).

33. We would like to thank our colleagues at the 1992 Ion Channels Gordon Conference for their helpful criticisms, J. Neyton for critically reviewing the manuscript, and A. Lee and E. Thomas for their continuing support throughout the course of this work. Supported by NIH grants GM43949 and GM47400.

28 July 1992; accepted 21 September 1992